Italian Association of Aeronautics and Astronautics
XXVII AIDAA International Congress
4-7 September 2023, Padova, Italy

Deployment profile analysis for tethered deorbiting technologies

G. Polato[1,a*], A. Valmorbida[1,2], A. Brunello[2], G. Anese[1], S. Chiodini[1,2], G. Colombatti[1,2], E.C. Lorenzini[1,2]

[1]University of Padova, Department of Industrial Engineering, Via Venezia 1, Padova, Italy

[2]University of Padova, Center for Studies and Activities for Space (CISAS) “Giuseppe Colombo”, Via Venezia 15, Padova, Italy

[a]giulio.polato@unipd.it

Keywords: tether deployment, optimization, deorbiting, clean space.

Abstract. Over the past few decades, the man-made space debris has become an increasingly concerning problem for future space missions. Fortunately, some innovative "green" deorbiting technologies have been emerged. Among these strategies, electrodynamic tethers have demonstrated to be a promising option, thanks to their passive and fuel-free characteristics. By leveraging the Earth's ionosphere and the geomagnetic field, an electrodynamic tether generates a Lorentz drag force, that can significantly reduce the altitude of a satellite and ultimately cause it to re-enter the atmosphere. The goal of this research is to investigate a critical part of satellite tethered technology, namely the deployment phase. To accomplish this, we utilized a software tool developed by the University of Padova to simulate the dynamics of the deployment phase and optimize its trajectory, in order to meet the desired boundary conditions. This paper gives a description of the software and shows the results of a sensitivity analysis on the trajectory profile that examines the impact of variations in the release angle of the tether and the speed profile actuated by the motor that controls the deployment speed.

Introduction

Tethered satellites technology has been studied for almost 60 years (first mission, Gemini 11 in 1966) [1]. These satellites can be used for many different purposes such as generating artificial gravity, electrical power generation or electrodynamic thrust [2]. One of the most critical part of a tethered satellite mission is the deployment phase. Depending on the purpose of the mission, the deployment profile followed by the tether, in order to meet the desired final conditions, must be carefully controlled. There are two possible ways to control the tether deployment: by imposing either a tension profile or a length/velocity profile on the reeled-out tether [3]. For the purpose of our study, we chose the second option, where a velocity profile is given as input to a motor that controls the angular velocity of a spool, where the tether is winded. The goal is to reach a final condition where the two satellite are aligned along the local vertical. The advantage of the second strategy is that the reel-out velocity can be more easily measured than the tension on a moving tether and also it can be accurately controlled by a motor with a feedback velocity control.

Mathematical model

The dynamic of tethered satellite is strongly non-linear and is influenced by several parameters. In order to reduce the complexity of the problem, we use a classical Dumbbell model for the system dynamics that assumes a rigid, straight, length-variable and mass-less tether [4]. The reference system and the parameters used are shown in Fig. 1.

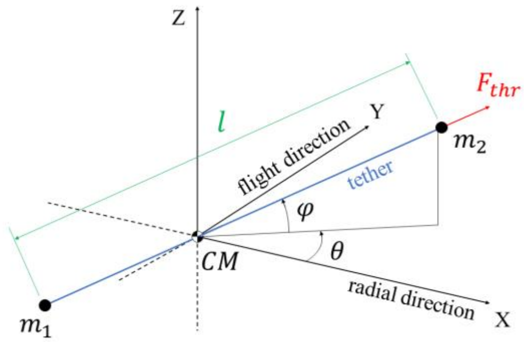

Fig. 1: Reference system frame for tethered satellite

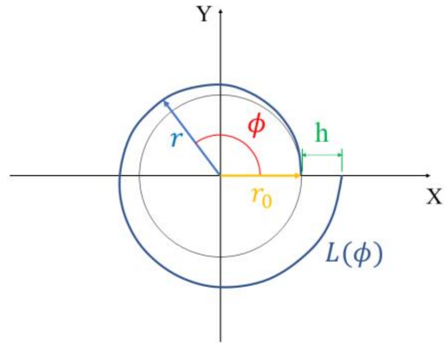

Fig. 2: Archimedean spiral parameters used to model the tape-shaped tether

The equations describing the deployment of a tethered system are the following:

$$\ddot{l} = l \cdot \left[(\dot{\theta} + \omega_O)^2 (\varphi) - \omega_O^2 + \varphi^2 + 3\,\omega_O^2 (\theta)\,(\varphi) \right] + \frac{F_{thr}}{m_2} - \frac{T_p}{m_R} \quad (1)$$

$$\ddot{\theta} = -2 \left[\frac{\dot{l}}{l} + \dot{\varphi}\, tan\, tan\,(\varphi) \right] (\dot{\theta} + \omega_O) + 3\,\omega_O^2\, cos\, cos\,(\theta)\;\, sin\, sin\,(\theta) \quad (2)$$

$$\ddot{\varphi} = -2\, m_R \frac{\dot{l}}{l} \dot{\varphi} - \left[(\dot{\theta} + \omega_O)^2 + 3\,\omega_O^2(\theta) \right] cos\, cos\,(\varphi)\;\, sin\, sin\,(\varphi) \quad (3)$$

where l is the tether length, θ the in-plane libration angle, φ the out-of-plane libration angle, F_{thr} the thrust applied on the second mass m_2, $m_R = \frac{m_1 m_2}{(m_1+m_2)}$ the reduced mass, T_p the tether tension, and ω_O the orbital angular velocity. For the reference deployment profile computation only the in-plane libration dynamics is considered $(\varphi, \dot{\varphi}, \ddot{\varphi} = 0)$; the out of plane oscillation is used only for the sensibility analysis.

Finally, in order to derive the control profile of the motor that extracts the tether from the stationary spool, we use the Archimedean spiral to model the tape-shaped tether winded on the spool [5] (see Fig. 2):

$$r = r_0 + \frac{h}{2\pi}\phi \quad (4)$$

$$L = \frac{h}{4\pi} \left[\phi \sqrt{\phi^2 + 1} + ln\, ln \left(\phi + \sqrt{\phi^2 + 1} \right) \right] \quad (5)$$

where r_0 is the initial radius, h the tether width, ϕ the angular coordinate of the spiral, $r(\phi)$ the radial coordinate of the spiral, and L the tether length in the spool varying from r_0 to r.

Software implementation

The software utilized for implementing the dynamics of the deployment was developed by the E.T.PACK-F team of the University of Padova. It mainly consists of four phases: the first three phases are used to derive the reference profile trajectory [6], and the last one is used to derive the input motor profile.

First Phase. In order to simulate the separation phase at the beginning of the deployment, we impose an acceleration profile driven by an initial thrust provided by the thrusters on board the module with mass m_2. As boundary conditions we imposed the maximum tether velocity that we want to reach and a time of 50 s needed to reach it. These values are compatible with the performance of the thrusters and the deployment motor.

Second Phase. During this phase, starting from the final conditions of the first phase, the trajectory is optimized using the software BOCOP [7], that approximates the optimal control problem with a finite-dimension optimization problem (NLP) through a time discretization. The boundary conditions to solve this problem are: the initial and final state conditions, i.e., tether length, length rate, libration angle and libration rate, the total deployment time, and upper and lower bounds of the state variables during the optimization process.

Third Phase. The last step for the trajectory profile derivation is to smooth out the transition between the first and the second phase, and the final part of the trajectory. This phase is important because we want to avoid sudden change in the acceleration profile, hence a sudden change in the tension of the tether that can lead to its rupture. In order to obtain a continuity of the second derivative (the acceleration) and a final acceleration equal to zero, we use an 8^{th}-order polynomial to approximate the length profile.

Fourth Phase: Finally, the velocity profile is converted to an angular velocity, using the Archimedean spiral model. The angular velocity is converted from deg/s to rpm which can be used as a reference profile for the motor that controls the spool mechanism.

Sensibility analysis

In order to study the stability of the reference trajectory we introduced errors in our simulations associated with the orientation misalignment of the modules at the beginning of the deployment ($\varepsilon_\theta = \pm 10\ deg, \varepsilon_\varphi = \pm 10\ deg$) on the in-plane and out-of-plane angles, respectively. In addition, we evaluated the influence of errors on the actual angular velocity of the deployment motor with respect to the reference profile ($\varepsilon_t = \pm 15\ deg/turns$), e.g., with an error of $\varepsilon_t = 9\ deg/turn$ the spool performs 1,025 turns instead of 1 turn, hence the motor is running faster than the reference velocity. The values considered for the ε_t error is exaggerated with respect to the actual performance of our motor, but we decided to use these values in order to have a better understanding of the general trend of the error.

The analysis was conducted by varying one driving variable at a time, in order to understand how each parameter affects the deployment dynamics and quantify its contribution to the error on the desired libration amplitude. For the demonstration flight of E.T.PACK-F, the requirement on the final libration amplitude is 10 deg [8].

Results

The following Fig. 3 show the results obtained while Table 1 summarizes the upper bounds of the limit cases. From the Fig. 3 it is possible to understand that the out-of-plane angle error has a smaller influence on the libration amplitude than the in-plane angle error.

Moreover from Fig. 4 it is shown the three trajectory obtained for the limit case of the three errors compared to the nominal trajectory. From this figure it is possible to visualize the effects of these three errors.

	ε_θ	ε_φ	ε_t
θ_{libr} lower bound error	0.9065 [deg]	$5.5247 \cdot 10^{-3}$ [deg]	-0.4385 [deg]
θ_{libr} upper bound error	-0.1651 [deg]	$0.1689 \cdot 10^{-3}$ [deg]	0.7656 [deg]

Table. 1 upper and lower bound error on the final libration angle

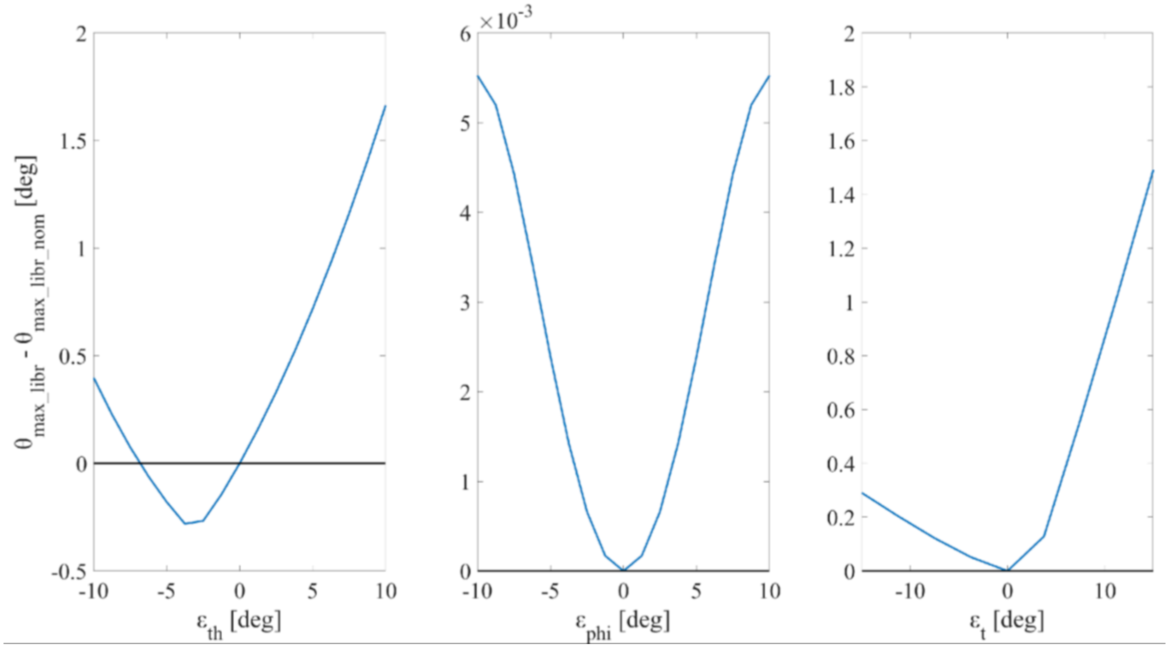

Fig. 3: Results of the sensibility analysis, where on the y-axis is indicated the difference between the free libration amplitude and the nominal libration amplitude

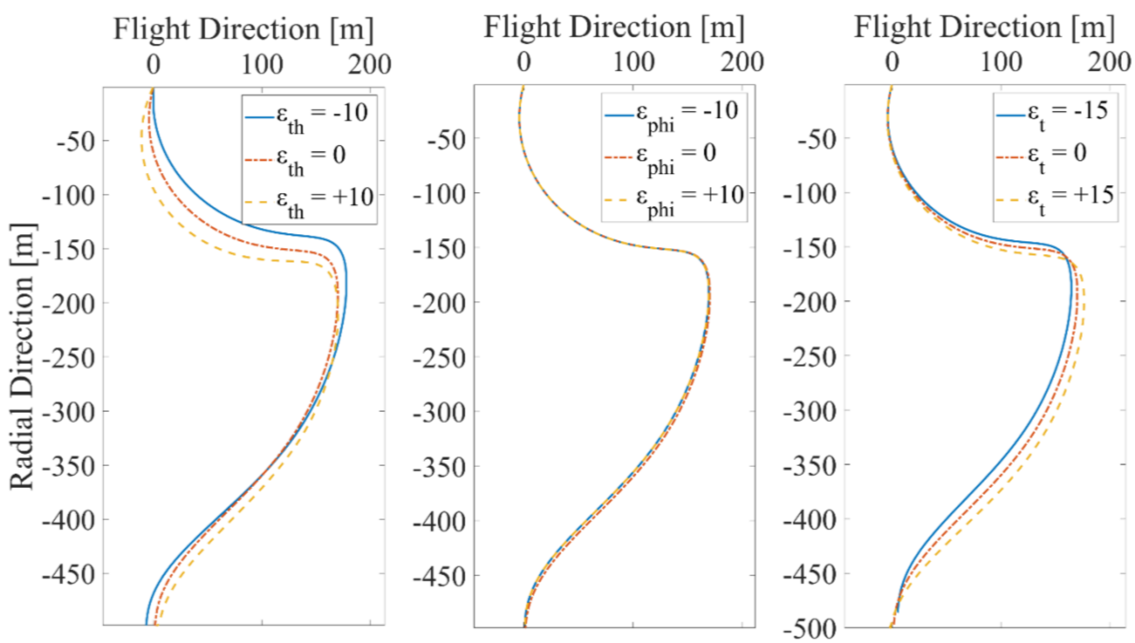

Fig. 4: Comparison of the trajectories for a the limit case of the three errors and the nominal trajectory

Finally, we can conclude also that having a higher velocity than the nominal brings to a higher error on the libration amplitude. Overall, the in-plane angle error has more influences on the libration amplitude, and it has the same order of error as the velocity error.

Conclusions

In this paper, we presented the software developed for the E.T.PACK-F project to compute the deployment reference trajectory and described the four phases of its operation. By considering initial and final conditions, we were able to determine an optimized trajectory that fulfills our deployment requirements. After that, we identified potential errors that could impact the post-deployment libration amplitude. To assess their influence, we conducted a sensitivity analysis evaluating the effects of each error individually. Based on the simulations conducted, we can conclude that the post-deployment libration amplitude is less than 2 deg, which satisfies the 10 deg requirement. This confirms that the computed reference trajectory for deployment shows a good robustness to the errors considered in this study.

Acknowledgments

This work was supported by Horizon Europe EIC Transition Programme under Grant Agreement No. 101058166 (E.T.PACK-F)

References

[1] Y. Chen, et al., History of the tether concept and tether missions: a review, International Scholarly Research Notices 2013 (2013). http://dx.doi.org/10.1155/2013/502973

[2] M. Kruijff, Tethers in Space: A propellantless propulsion in-orbit demonstration., Ph.D. Thesis, Technical Univ. of Delft, Delft, The Netherlands, (2011).

[3] E. C. Lorenzini, et al., Control and flight performance of tethered satellite small expendable deployment system-II, Journal of Guidance, Control, and Dynamics 19.5 (1996): 1148-1156. https://doi.org/10.2514/3.21757

[4] P. Mantri, Deployment Dynamic of Space Tether Systems, Ph.D. Thesis, Faculty of North Carolina State University (2007).

[5] from: https://en.wikipedia.org/wiki/Archimedean_spiral

[6] from: https://research.dii.unipd.it/mts/

[7] Team Commands, I. Saclay, BOCOP: an open-source toolbox for optimal control. (2017), See: http://bocop.org

[8] G. Sarego, et al., Deployment requirements for deorbiting electrodynamic tether technology, CEAS Space Journal 13.4 (2021): 567-581.